

pubs.acs.org/NanoLett Letter

# Nonreciprocal Transmission of Incoherent Magnons with Asymmetric Diffusion Length

Jiahao Han,\* Yabin Fan, Brooke C. McGoldrick, Joseph Finley, Justin T. Hou, Pengxiang Zhang, and Luqiao Liu\*



Cite This: Nano Lett. 2021, 21, 7037-7043



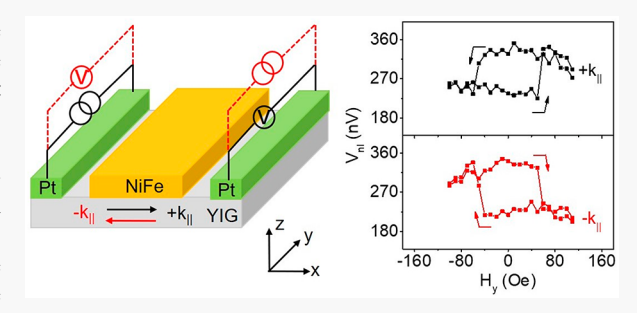
**ACCESS** 

Metrics & More

Article Recommendations

Supporting Information

ABSTRACT: Unequal transmissions of spin waves along opposite directions provide useful functions for signal processing. So far, the realization of such nonreciprocal spin waves has been mostly limited at a gigahertz frequency in the coherent regime via microwave excitation. Here we show that, in a magnetic bilayer stack with chiral coupling, tunable nonreciprocal propagation can be realized in spin Hall effect-excited incoherent magnons, whose frequencies cover the spectrum from a few gigahertz up to terahertz. The sign of nonreciprocity is controlled by the magnetic orientations of the bilayer in a nonvolatile manner. The nonreciprocity is further verified by measurements of the magnon diffusion length, which is unequal along opposite transmission



directions. Our findings enrich the knowledge on magnetic relaxation and diffusive transport and can lead to the design of a passive directional signal isolation device in the diffusive regime.

KEYWORDS: nonreciprocity, incoherent magnons, asymmetric magnon diffusion length, nonlocal transport

ne of the important applications of magnetic materials in information processing and communication is to provide the function of nonreciprocity. Driven by the need for highperformance, compact nonreciprocal devices, new mechanisms that can provide passive, directional isolation of signals are being pursued at the submicrometer scale, among which spin waves show unique potentials due to the tunability and the possibility for on-chip integration. In literature, nonreciprocal spin waves have been achieved through the magnetostatic surface mode<sup>2-4</sup> or by asymmetrically modifying the spin wave dispersion under the effect of the Dzyaloshinskii-Moriya interaction (DMI).<sup>5-9</sup> Most recently, the dipolar coupling between different magnetic layers has been studied for nonreciprocity, where the dispersion relation is shifted asymmetrically or the spin wave mode is excited directionally. 10-14 However, these nonreciprocal effects are limited to coherent spin waves under single frequencies in the ballistic regime. It remains elusive whether the nonreciprocity can be reached for incoherent, diffusive magnons that occupy a broadband spectrum.

In this work, with a bilayer composed of a ferrimagnetic insulator  $Y_3Fe_5O_{12}$  (YIG) and a magnetic alloy NiFe, we find that the diffusion of the spin Hall effect (SHE)-induced incoherent magnons has unequal transmission coefficients along opposite directions. We further verify that the non-reciprocal transmission is caused by the asymmetric magnon diffusion length controlled by the magnetic moment configuration. This work provides an efficient mechanism for

designing passive devices with directional signal isolation that works in the diffusive regime.

The device structure in our experiment is shown in Figure 1a,b (see Supporting Information Section 1 for materials and methods). A 50 nm thick YIG film (resistivity >  $10^{12} \mu\Omega$  cm, Gilbert damping ~ 10<sup>-4</sup>) is deposited on Gd<sub>3</sub>Ga<sub>5</sub>O<sub>12</sub> substrates. A pair of Pt electrodes are fabricated to inject and detect magnon flow. 15-19 A NiFe strip (40 nm thick) is deposited on YIG between the two Pt electrodes and is electrically isolated with other electrodes. During the measurement, a low-frequency (<50 Hz) alternating current is applied on the Pt injector to excite broadband magnons via the SHE. The nonequilibrium magnons diffuse toward the Pt detector and get converted to a charge current via the inverse SHE, which is probed by the first harmonic voltage using a lock-in amplifier at room temperature. 15,19 In a device without the NiFe strip, the nonlocal voltage  $V_{\rm nl}$  exhibits a  $\sin^2 \varphi$ dependence on the angle  $\varphi$  of the in-plane applied field H(Figure 1c), consistent with the previous observations, confirming the SHE-induced magnon excitation/detection mechanism. In Figure 1c,  $\pm k_{\parallel}$  denotes right-/left-going

Received: July 1, 2021 Revised: August 4, 2021 Published: August 10, 2021





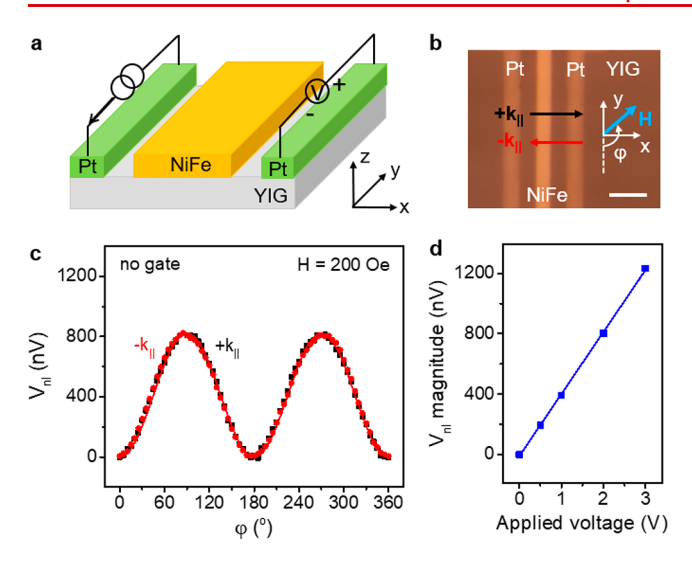


**Figure 1.** Device structure and basic nonlocal transport properties. (a) Schematic of a nonlocal device consisting of a YIG layer with two Pt electrodes and a NiFe strip on top. (b) Optical image of a device. The scale bar is 5  $\mu$ m. (c) Angular dependence of  $V_{\rm nl}$  in a device without the NiFe strip under an applied field of 200 Oe. The solid line is sinusoidal fitting. (d) Magnitude of the nonlocal voltage as a function of the applied voltage. The solid line is linear fitting.

magnon flow, which is experimentally realized by swapping the role of injection/detection Pt electrodes. The magnitude of  $V_{\rm nl}$  scales linearly with the applied voltage (Figure 1d), suggesting that the magnon excitation is in the linear response regime.

Because of the long strip shape, the NiFe layer has an inplane uniaxial anisotropy with an easy axis along the ydirection, as is verified by the measurement on the anisotropic magnetoresistance (AMR) of the NiFe strip (Supporting Information Section 2). This shape anisotropy tends to tilt the magnetic moment  $m_{\text{NiFe}}$  away from the applied field toward the easy axis. In contrast, the YIG moment  $m_{\text{YIG}}$  more closely follows the field orientation due to the negligible anisotropy. Consequently,  $m_{\text{YIG}}$  and  $m_{\text{NiFe}}$  generally have a misalignment angle under a finite applied field, which is critical for causing nonreciprocal magnon transmission in the considered system (discussed later).

We now study the angular dependence of magnon transmission under the influence of NiFe. We measure  $V_{\rm nl}$ by rotating a field of 200 Oe within the film plane (Figure 2a). We notice that compared with the  $\sin^2 \varphi$  dependence shown in the single-layer YIG sample of Figure 1c, the existence of NiFe significantly distorts the line shape. Moreover, a nonreciprocity emerges in the magnon transmission, i.e., under the same field condition, the magnitude of transmission coefficient changes when one switches the magnon flowing direction. This nonreciprocity is most significant for  $\varphi$  around 90° and 270°. By comparing with the AMR data of NiFe, we can correlate the sudden jump of  $V_{\rm nl}$  at  $\sim 100^{\circ}$  and  $\sim 280^{\circ}$  with the flipping of the y component of  $m_{NiFe}$ . It can be seen that the nonreciprocity ratio  $\xi = [V_{\rm nl}(+k_{\parallel}) - V_{\rm nl} (-k_{\parallel})]/{\rm max}(V_{\rm nl})$ changes sign when  $\emph{m}_{\mathrm{NiFe}}$  switches, with  $\xi$  being negative for  $\phi$ < 100° or >280° (regions I and IV) and positive otherwise (regions II and III). Here  $max(V_{nl})$  is the higher value between  $V_{\rm nl}(+k_{\parallel})$  and  $V_{\rm nl}(-k_{\parallel})$  for normalization purposes. For a better comparison, we schematically illustrate in Figure 2b the orientations of  $m_{NiFe}$  and  $m_{YIG}$  for the four different regions of  $\varphi = 0-360^{\circ}$ . The magnon transmission is also studied under a larger rotating field of 800 Oe, which aligns  $m_{NiFe}$  closer to the field direction and reduces the misalignment between  $m_{\rm NiFe}$ and  $m_{YIG}$ . As plotted in Figure 2c, despite the absence of abrupt jump and a smaller overall magnitude,  $V_{\rm nl}$  exhibits

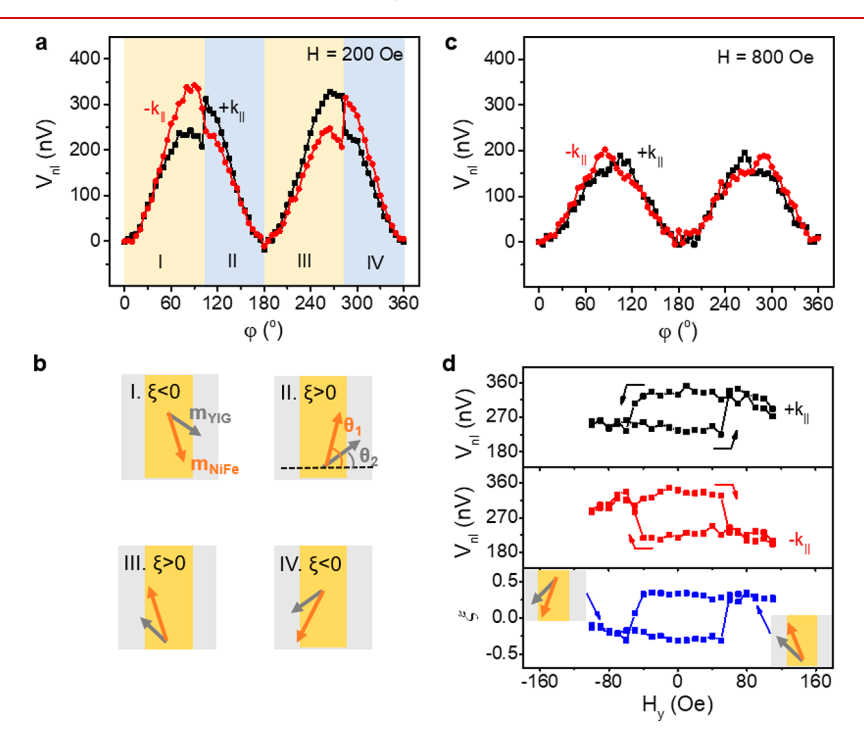


Figure 2. Nonlocal voltage in YIG gated by a 1  $\mu$ m wide NiFe strip. (a) Angular dependence of  $V_{\rm nl}$  for  $\pm k_{\parallel}$  magnon flows under an applied field of 200 Oe. (b) Schematic of  $m_{\rm NiFe}$  and  $m_{\rm YIG}$  orientations for different regions labeled in panel a. (c) Angular dependence of  $V_{\rm nl}$  under an applied field of 800 Oe. (d) Top and middle panels:  $V_{\rm nl}$  as a function of  $H_y$  for  $\pm k_{\parallel}$  magnon flows. A fixed field of  $H_x = -200$  Oe is applied. Bottom panel: nonreciprocity ratio  $\xi$  as a function of  $H_y$ . The schematics illustrate the directions of  $m_{\rm NiFe}$  and  $m_{\rm YIG}$  under positive and negative values of  $H_y$ .

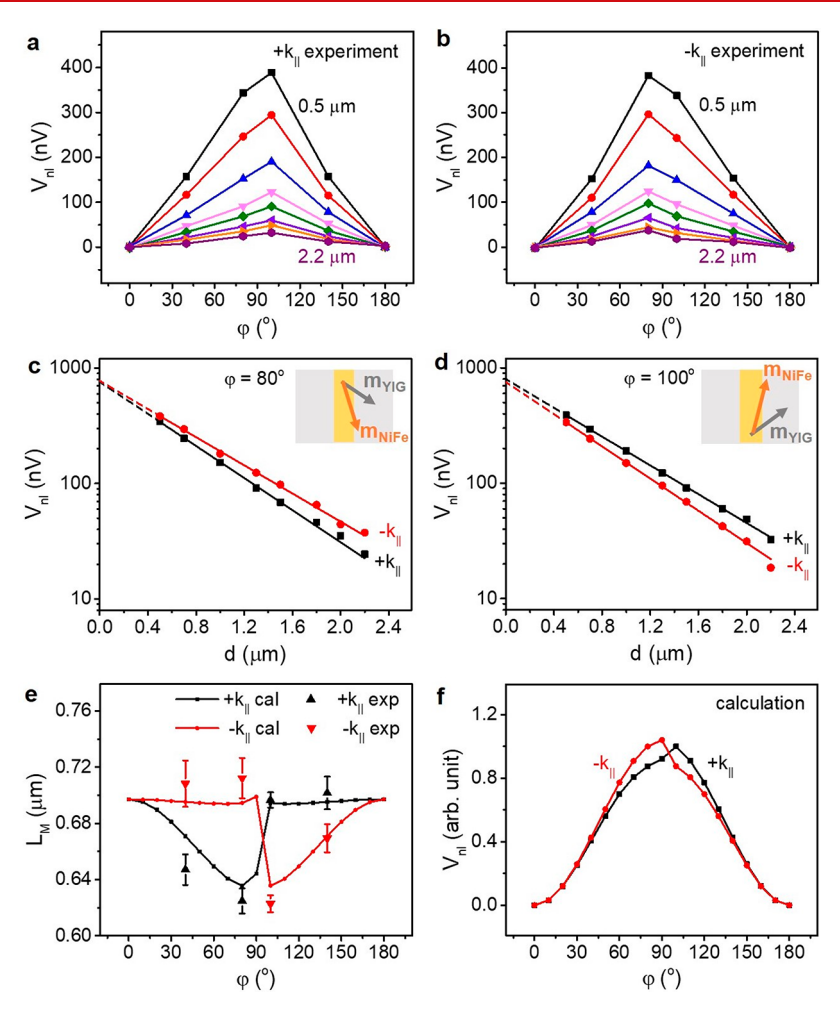


Figure 3. Magnon transmission with asymmetric diffusion lengths. (a, b) Measured  $V_{\rm nl}$  as a function of field angle  $\varphi$  for  $\pm k_{\parallel}$  magnon flows with different NiFe widths d. The curves from top to bottom correspond to  $d=0.5,0.7,1.0,1.3,1.5,1.8,2.0.2.2~\mu{\rm m}$ . (c, d) Fitting of  $V_{\rm nl}$  as a function d at  $\varphi=80^{\circ}$  and  $100^{\circ}$ . The lines are exponential fittings. (e) Magnon diffusion length  $L_{\rm M}$  for  $\pm k_{\parallel}$  magnon flows as a function of the field angle. The dots represent the result from experiments shown in panels a and b, with error bars representing the standard error of the mean (S.E.M.) from the fitting. The lines are calculated from the analytical modeling. (f) Calculated angular dependence of  $V_{\rm nl}$  in a device with a 1  $\mu{\rm m}$  wide NiFe strip. Both experiment and modeling of this figure are carried out under H=800 Oe.

qualitatively the same nonreciprocity as Figure 2a. The smaller  $V_{\rm nl}$  compared with the 200 Oe case can be explained by the suppression of magnon excitation under a large field. On the basis of the sign of  $\xi$  and the fact that the nonreciprocity is stronger when the misalignment between the two moment vectors is larger, we summarize an empirical relation for nonreciprocity as  $\xi \propto \hat{z} \cdot [\hat{x} \times (m_{\rm NiFe} - m_{\rm YIG})]$ , which shows that a finite difference between the two magnetic moments along the y axis is the key to cause and manipulate the nonreciprocity. This is distinct from the previous studies on modulating magnon current with magnetic electrodes, where nonreciprocity is not observed as the field is either purely applied along the x axis  $^{21}$  or is too large, which aligns the two magnetic layers almost perfectly parallel with each other.

The correlation between the nonreciprocity on  $V_{\rm nl}$  and  $m_{\rm NiFe}$  suggests that one can realize nonreciprocal magnon diffusion in a tunable, nonvolatile manner. To show this point, besides field rotation measurements, we also measure the  $V_{\rm nl}$  hysteresis loops by sweeping a field along the y axis for  $\pm k_{\rm ll}$  configurations (top and middle panels of Figure 2d). Limited by the  $\sin^2\!\phi$  dependence from the SHE-induced magnon excitation and detection, on top of the sweeping field along the y axis, we have to apply a constant field along the x axis to maintain a finite

 $V_{\rm nl}$ . Nevertheless, we note that in the bistable region, by controlling the field sweeping history, one can reach desired nonreciprocity with positive or negative  $\xi$  under the same  $H_y$  (bottom panel of Figure 2d), which effectively demonstrates the function of a nonvolatile, nonreciprocal magnon transistor.

A more detailed study shows that the observed nonreciprocal transmission is related to the asymmetric magnon diffusion length along opposite directions under specific magnetic moment configurations. To show this, we vary the NiFe strip width d between 0.5 and 2.2  $\mu$ m, and measure  $V_{\rm nl}$ under each applied field angle (Figure 3a,b for  $\pm k_{\parallel}$ ), respectively). In this measurement, we use a high magnetic field of 800 Oe to minimize the influence from the shape anisotropy and magnetic domain switching of the NiFe strip. From Figure 3a,b, we can see that, for all of the studied samples, the angle dependence of  $V_{\rm nl}$  shows the same asymmetry as that in Figure 2, suggesting that the nonreciprocity is qualitatively consistent regardless of the strip widths. We summarize  $V_{\rm nl}(\pm k_{\parallel})$  as a function of the gate width d under each fixed applied field. As an example, in Figure 3c,d for  $\varphi = 80^{\circ}$  and  $100^{\circ}$ , the gate width dependence of  $V_{\rm nl}$  can be fitted with an exponential relationship of  $V_{\rm nl}(d) \propto \exp(-d/d)$  $L_{\rm M}$ ), <sup>16</sup> where  $L_{\rm M}$  denotes the magnon diffusion length. As d

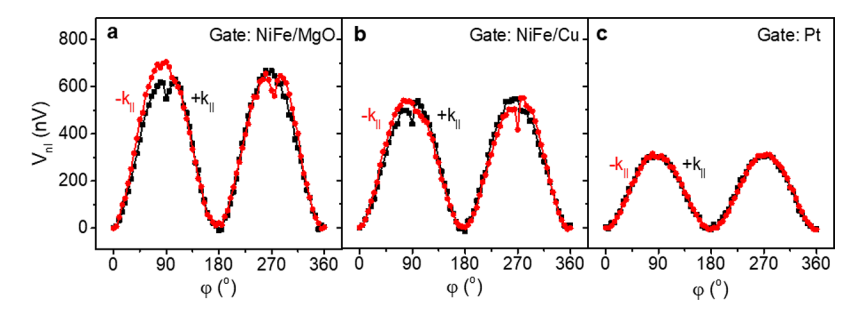


Figure 4. Angular dependence of the nonlocal voltage in devices with different gates: (a) NiFe (40)/MgO (3), (b) NiFe (40)/Cu (8), and (c) Pt (10) (unit in nm). The gate widths are kept at 1  $\mu$ m. The applied field is 200 Oe.

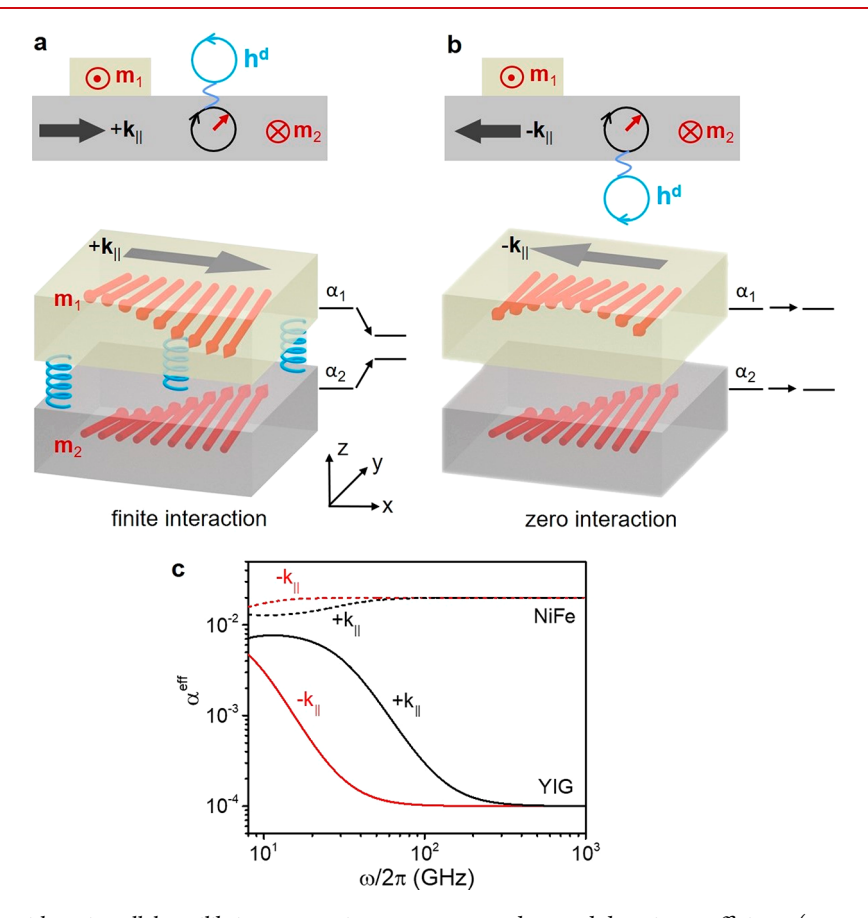


Figure 5. Magnetic bilayer with antiparallel equilibrium magnetic moments  $m_1$  and  $m_2$  and damping coefficients ( $\alpha_1 > \alpha_2$ ). (a) For the right-going ( $+k_{\parallel}$ ) spin wave, the dynamic dipolar field ( $h^d$ ) generated from the magnetic oscillation of the bottom layer appears at its upper side. The two layers are coupled through dynamic dipolar interactions, resulting in a modulation of damping coefficients. (b) For the left-going ( $-k_{\parallel}$ ) spin wave,  $h^d$  from the magnetic oscillation of the bottom layer appears at its lower side, which does not induce the dynamic interlayer dipolar coupling. The damping factors of the two layers remain unchanged. (c) Calculated magnon attenuation rates of NiFe and YIG as a function of frequency for  $\pm k_{\parallel}$  configurations when an 800 Oe field is applied along  $\varphi = 80^{\circ}$  direction.

varies, the magnetic shape anisotropy of NiFe also changes. However, in our studied samples, the antiferromagnetic exchange interaction at NiFe/YIG interface plays an important role in maintaining the misalignment angle, leading to the consistent scaling behavior observed here. After extracting  $L_{\rm M}$  for different field angles for the two propagation directions, we summarize  $L_{\rm M}(\pm k_{\parallel})$  in Figure 3e (solid dots), which show a clear difference between  $\pm k_{\parallel}$  directions, confirming the nonreciprocal magnon diffusion.

In a magnetically gated spin wave channel device, several factors can potentially influence the magnon transmission, including the interactions due to the interfacial exchange, spin transfer across the interface, the DMI, as well as the interlayer

dipolar coupling. To understand their potential contributions to the observed nonreciprocal magnon transmission, we carry out experiments with control samples. First, to study the role of interfacial exchange, we make samples by inserting a spacer layer of 3 nm MgO or 8 nm Cu between NiFe and YIG. Both spacers can eliminate the interlayer exchange interaction, while the MgO also blocks the spin current from YIG to NiFe. <sup>23,26</sup> As shown in Figure 4a,b, a weaker but finite nonreciprocity with the same sign as the NiFe/YIG device is observed. The persistence of nonreciprocity suggests that the interlayer exchange interaction and the possible spin current absorption at the top surface of YIG cannot be the dominant origin of the observed nonreciprocity. On the other hand, the non-

reciprocity ratio of the NiFe/YIG device is more than two times larger than that of the MgO and Cu control samples. This is because the antiferromagnetic exchange interaction between NiFe and YIG increases the misalignment angle of the equilibrium magnetic moments of the two layers,  $^{23-25,27}$  which is beneficial for achieving high nonreciprocity in our studied system, as discussed earlier. Besides the classical exchange interaction, it is known that the interfacial DMI can lead to asymmetries in the dispersion relation to cause nonreciprocal spin wave transmission. To understand the possible role played by DMI in our system, we replace the center NiFe strip with nonmagnetic Pt. As plotted in Figure 4c, the difference between  $V_{\rm nl}(\pm k_{\parallel})$  is far less observable compared with the NiFe/YIG device, which suggests that the DMI itself cannot lead to the strong nonreciprocity shown in Figure 2.

The continuing existence of nonreciprocal magnon transmission even in the absence of a direct contact between NiFe and YIG suggests that the effect comes from certain long-range interactions. Recently, it was theoretically demonstrated that the interactions caused by dynamic magnetic dipolar fields in magnetic multilayers can lead to nonreciprocal excitations of spin wave modes. This interaction works efficiently both for coherent and incoherent magnons. 10 While ref 10 considers the interaction between a two-dimensional thin film and a quasi-one-dimensional nanowire, we can extend the model to bilayer films with both layers being extended (see Supporting Information Section 4). As shown in ref 10, due to its chiral nature, the dynamic dipolar field generated from magnons in a thin film magnet is single-sided; i.e., it can have finite or zero magnitude at the neighboring film location, depending on the magnon propagation direction (Figure 5a,b). Correspondingly, in a bilayer with antiparallel magnetizations, the magnon modes of the two layers will have finite interaction for  $+ k_{\parallel}$ (Figure 5a) but no interaction for  $-k_{\parallel}$  (Figure 5b). As a result, the magnon modes of the two layers, hence their attenuation rates, are hybridized for +  $k_{\parallel}$ , while remaining largely unchanged from their intrinsic value for  $-k_{\parallel}$ . Since the intrinsic damping values of the two layers in our experiment are very different (in the order of  $10^{-4}$  and  $10^{-2}$  for YIG and NiFe, respectively), the resulted magnon attenuation rate becomes highly asymmetric with respect to the wavevector direction, i.e.,  $\alpha^{\text{eff}}(+k_{\parallel}) \neq \alpha^{\text{eff}}(-k_{\parallel})$ . In our real experiment, the equilibrium magnetic moments are not perfectly antiparallel, but the dipolar fields still lead to unequal magnon interactions and thus unequal magnon attenuation rates for opposite directions, but with smaller asymmetry. An analytical evaluation of the magnon attenuation rate is provided in Supporting Information Section 5, and the calculated results under a typical magnetic configuration are plotted in Figure 5c.

To account for the influence of direction-dependent attenuation rates on the diffusion of incoherent magnons, one can solve the Boltzmann transport equation and sum over all of the thermally populated modes. We obtain a diffusion equation for the quasi-equilibrium magnon chemical potential  $\mu$ :  $2^{8-30}$ 

$$\sigma \frac{\partial^2 \mu}{\partial x^2} + \delta \frac{\partial \mu}{\partial x} - \eta \mu = 0 \tag{1}$$

The first and third terms of eq 1 correspond to the divergence of magnon current density and the conventional magnon relaxation, with  $\sigma$  and  $\eta$  being proportional to the magnon conductivity and spin nonconserving scattering rate,

as in the standard continuity equation for diffusion. <sup>28,29</sup> The second term is a new one that accounts for the asymmetric attenuation, where  $\delta$  originates from integrating the directiondependent magnon attenuation rate  $\alpha^{\text{eff}}(\mathbf{k}_{\parallel})$  of YIG over all possible directions in the xy plane, weighted by magnons' distribution function and their corresponding group velocity (see Supporting Information Section 6 for derivation). The solution of eq 1 has the form of  $\mu_{\pm} \propto \exp(\mp x/L_{\rm M\pm})$ , with  $L_{\rm M+} = [\mp \delta + \sqrt{\delta^2 + 4\eta\sigma}]/2\eta$  representing the magnon diffusion length along the  $\pm x$  axes. Using material parameters that are consistent with our structure, we calculate  $L_{\mathrm{M+}}$  under an applied field of 800 Oe and plot the result as solid lines in Figure 3e as a function of the field angle, showing the same trend as the experimental values.  $V_{\rm nl}$ , which is proportional to  $\mu_{+}$  for a given distance of  $d = 1 \mu m$ , is plotted in Figure 3f, exhibiting similar nonreciprocal behaviors as the experimental result in Figure 2c.

To further verify the critical role of the interlayer dipolar coupling-modulated magnon attenuation, we consider two magnetic layers with identical intrinsic damping in the modeling, where the resultant asymmetry in the magnon attenuation rate will be less profound. We obtain a much weaker nonreciprocity in this case, confirming that the imaginary part of the hybridized magnon dispersion, i.e., the magnon attenuation rate, rather than its real part, is the main source of the observed nonreciprocal phenomena (see Supporting Information Figure S6). Furthermore, we verify this asymmetric magnon attenuation with micromagnetic simulations, where we consider the detailed device geometry and obtain the same nonreciprocity (Supporting Information Section 7). We also note that under the mechanism of interlayer dipolar coupling, the nonreciprocity can benefit from a relatively thick NiFe because a large number of magnetic moments couples with YIG, whereas a very thin magnetic gate can make the nonreciprocity less profound.<sup>22</sup>

Before ending, we address a seeming paradox associated with the lock-in measurement of magnon transmission. Under an alternating driving current, the SHE enhances local magnon population under the Pt injector for a one-half period while suppressing it for the other. 15 It is tempting to think that magnons transmit along opposite directions in the two half periods, and the asymmetric magnon relaxation effect averages out. The key point for understanding this is that the enhanced or suppressed magnon population is in reference to their thermal equilibrium value. 15,31 Since the thermal equilibrium state corresponds to zero net magnon flow, it is convenient to treat the suppressed magnons as deficiencies from equilibrium, which flow away from the injector and experience the same attenuation rate as the excessive magnons in the other half period. Mathematically, the modulated magnon population is reflected in the sign of  $\mu$  in eq 1, with a negative  $\mu$ corresponding to the case of magnon deficiency. The choice of  $L_{\mathrm{M+}}$  depends on the relative location of the injector and detector electrodes, rather than the sign of  $\mu$ . Thus, the observation of a nonreciprocity between  $\pm k_{\parallel}$  is expected for the lock-in measurement configuration.

In conclusion, we demonstrate the nonreciprocal transmission of the SHE-excited incoherent magnons in a magnetically gated ferrimagnetic insulator channel through nonlocal charge-transfer measurements. The sign of nonreciprocity is switchable by magnetic fields through the control of the bilayer's magnetic orientation. The magnon diffusion

length is asymmetric over the transmission direction. This nonreciprocal magnon diffusion can be explained by the asymmetric magnon attenuation rate induced by the interlayer dipolar coupling. For future applications, one can potentially utilize magnetic materials with even larger differences in damping to enlarge the asymmetry in magnon attenuation, which will enhance the nonreciprocity. For example, YIG films with an ultralow damping of  $5.2 \times 10^{-5}$  have been reported in recent literature, <sup>32</sup> which is ideal for maximizing the hybridization effect of magnon attenuation rates. An even useful device with electrically programmable directional signal isolation can also be achieved by integrating our device with voltage- or current-induced switching of the magnetic gate. <sup>33,34</sup>

# ASSOCIATED CONTENT

# **Supporting Information**

The Supporting Information is available free of charge at https://pubs.acs.org/doi/10.1021/acs.nanolett.1c02575.

Materials and methods, anisotropic magnetoresistance of NiFe strip, hysteresis of nonreciprocal magnon transmission detailed explanation of the interlayer dipolar coupling, calculation of the asymmetric magnon attenuation rate, integration on the Boltzmann transport equation, and micromagnetic simulations (PDF)

## AUTHOR INFORMATION

## **Corresponding Authors**

Jiahao Han — Department of Electrical Engineering and Computer Science, Massachusetts Institute of Technology, Cambridge, Massachusetts 02139, United States; Email: jhhan@mit.edu

Luqiao Liu — Department of Electrical Engineering and Computer Science, Massachusetts Institute of Technology, Cambridge, Massachusetts 02139, United States;
occid.org/0000-0001-6892-8102; Email: luqiao@mit.edu

### **Authors**

Yabin Fan — Department of Electrical Engineering and Computer Science, Massachusetts Institute of Technology, Cambridge, Massachusetts 02139, United States

Brooke C. McGoldrick – Department of Electrical Engineering and Computer Science, Massachusetts Institute of Technology, Cambridge, Massachusetts 02139, United States

Joseph Finley – Department of Electrical Engineering and Computer Science, Massachusetts Institute of Technology, Cambridge, Massachusetts 02139, United States

Justin T. Hou – Department of Electrical Engineering and Computer Science, Massachusetts Institute of Technology, Cambridge, Massachusetts 02139, United States

Pengxiang Zhang – Department of Electrical Engineering and Computer Science, Massachusetts Institute of Technology, Cambridge, Massachusetts 02139, United States

Complete contact information is available at: https://pubs.acs.org/10.1021/acs.nanolett.1c02575

### Notes

The authors declare no competing financial interest.

## ACKNOWLEDGMENTS

We thank Weichao Yu for fruitful discussions. This work is supported by AFOSR under award no. FA9550-19-1-0048, National Science Foundation under award no. ECCS-1808826, and SMART, one of seven centers of nCORE, a Semiconductor Research Corporation program, sponsored by the National Institute of Standards and Technology.

## REFERENCES

- (1) Li, Y.; Zhang, W.; Tyberkevych, V.; Kwok, W.-K.; Hoffmann, A.; Novosad, V. Hybrid magnonics: Physics, circuits, and applications for coherent information processing. *J. Appl. Phys.* **2020**, *128*, 130902.
- (2) Jamali, M.; Kwon, J. H.; Seo, S.-M.; Lee, K.-J.; Yang, H. Spin wave nonreciprocity for logic device applications. *Sci. Rep.* **2013**, *3*, 3160.
- (3) An, T.; Vasyuchka, V. I.; Uchida, K.; Chumak, A. V.; Yamaguchi, K.; Harii, K.; Ohe, J.; Jungfleisch, M. B.; Kajiwara, Y.; Adachi, H.; Hillebrands, B.; Maekawa, S.; Saitoh, E. Unidirectional spin-wave heat conveyer. *Nat. Mater.* **2013**, *12*, 549–553.
- (4) Wong, K. L.; Bi, L.; Bao, M.; Wen, Q.; Chatelon, J. P.; Lin, Y.-T.; Ross, C. A.; Zhang, H.; Wang, K. L. Unidirectional propagation of magnetostatic surface spin waves at a magnetic film surface. *Appl. Phys. Lett.* **2014**, *105*, 232403.
- (S) Nembach, H. T.; Shaw, J. M.; Weiler, M.; Jué, E.; Silva, T. J. Linear relation between Heisenberg exchange and interfacial Dzyaloshinskii-Moriya interaction in metal films. *Nat. Phys.* **2015**, *11*, 825–829.
- (6) Zakeri, K.; Zhang, Y.; Prokop, J.; Chuang, T.-H.; Sakr, N.; Tang, W. X.; Kirschner, J. Asymmetric spin wave dispersion on Fe(110): direct evidence of the Dzyaloshinskii-Moriya interaction. *Phys. Rev. Lett.* **2010**, *104*, 137203.
- (7) Lee, J. M.; Jang, C.; Min, B.-C.; Lee, S.-W.; Lee, K.-J.; Chang, J. All-electrical measurement of interfacial Dzyaloshinskii-Moriya interaction using collective spin-wave dynamics. *Nano Lett.* **2016**, 16, 62–67
- (8) Wang, H.; Chen, J.; Liu, T.; Zhang, J.; Baumgaertl, K.; Guo, C.; Li, Y.; Liu, C.; Che, P.; Tu, S.; Liu, S.; Gao, P.; Han, X.; Yu, D.; Wu, M.; Grundler, D.; Yu, H. Chiral spin-wave velocities induced by allgarnet interfacial Dzyaloshinskii-Moriya interaction in ultrathin yttrium iron garnet films. *Phys. Rev. Lett.* **2020**, *124*, 027203.
- (9) Lan, J.; Yu, W.; Wu, R.; Xiao, J. Spin-wave diode. *Phys. Rev. X* **2015**, *5*, 041049.
- (10) Yu, T.; Blanter, Y. M.; Bauer, G. E. W. Chiral pumping of spin wave. *Phys. Rev. Lett.* **2019**, 123, 247202.
- (11) Yu, T.; Liu, C.; Yu, H.; Blanter, Y. M.; Bauer, G. E. W. Chiral excitation of spin waves in ferromagnetic films by magnetic nanowire gratings. *Phys. Rev. B: Condens. Matter Mater. Phys.* **2019**, 99, 134424.
- (12) Chen, J.; Yu, T.; Liu, C.; Liu, T.; Madami, M.; Shen, K.; Zhang, J.; Tu, S.; Alam, M. S.; Xia, K.; Wu, M.; Gubbiotti, G.; Blanter, Y. M.; Bauer, G. E. W.; Yu, H. Excitation of unidirectional exchange spin waves by a nanoscale magnetic grating. *Phys. Rev. B: Condens. Matter Mater. Phys.* **2019**, *100*, 104427.
- (13) Gallardo, R. A.; Schneider, T.; Chaurasiya, A. K.; Oelschlägel, A.; Arekapudi, S. S. P. K.; Roldán-Molina, A.; Hübner, R.; Lenz, K.; Barman, A.; Fassbender, J.; Lindner, J.; Hellwig, O.; Landeros, P. Reconfigurable spin-wave nonreciprocity induced by dipolar interaction in a coupled ferromagnetic bilayer. *Phys. Rev. Appl.* **2019**, *12*, 034012.
- (14) Ishibashi, M.; Shiota, Y.; Li, T.; Funada, S.; Moriyama, T.; Ono, T. Switchable giant nonreciprocal frequency shift of propagating spin waves in synthetic antiferromagnets. *Sci. Adv.* **2020**, *6*, eaaz6931.
- (15) Cornelissen, L. J.; Liu, J.; Duine, R. A.; Youssef, J. B.; van Wees, B. J. Long-distance transport of magnon spin information in a magnetic insulator at room temperature. *Nat. Phys.* **2015**, *11*, 1022–1026.
- (16) Giles, B. L.; Yang, Z.; Jamison, J. S.; Myers, R. C. Long-range pure magnon spin diffusion observed in a nonlocal spin-Seebeck

- geometry. Phys. Rev. B: Condens. Matter Mater. Phys. 2015, 92, 224415.
- (17) Wesenberg, D.; Liu, T.; Balzar, D.; Wu, M.; Zink, B. L. Long-distance spin transport in a disordered magnetic insulator. *Nat. Phys.* **2017**, *13*, 987–993.
- (18) Ross, A.; Lebrun, R.; Gomonay, O.; Grave, D. A.; Kay, A.; Baldrati, L.; Becker, S.; Qaiumzadeh, A.; Ulloa, C.; Jakob, G.; Kronast, F.; Sinova, J.; Duine, R.; Brataas, A.; Rothschild, A.; Kläui, M. Propagation length of antiferromagnetic magnons governed by domain configurations. *Nano Lett.* **2020**, *20*, 306–313.
- (19) Han, J.; Zhang, P.; Bi, Z.; Fan, Y.; Safi, T. S.; Xiang, J.; Finley, J.; Fu, L.; Cheng, R.; Liu, L. Birefringence-like spin transport via linearly polarized antiferromagnetic magnons. *Nat. Nanotechnol.* **2020**, *15*, 563–568.
- (20) Cornelissen, L. J.; van Wees, B. J. Magnetic field dependence of the magnon spin diffusion length in the magnetic insulator yttrium iron garnet. *Phys. Rev. B: Condens. Matter Mater. Phys.* **2016**, 93, 020403.
- (21) Das, K. S.; Feringa, F.; Middelkamp, M.; van Wees, B. J.; Vera-Marun, I. J. Modulation of magnon spin transport in a magnetic gate transistor. *Phys. Rev. B: Condens. Matter Mater. Phys.* **2020**, *101*, 054436.
- (22) Wimmer, T.; Coester, B.; Geprägs, S.; Gross, R.; Goennenwein, S. T. B.; Huebl, H.; Althammer, M. Anomalous spin Hall angle of a metallic ferromagnet determined by a multiterminal spin injection/detection device. *Appl. Phys. Lett.* **2019**, *115*, 092404.
- (23) Fan, Y.; Quarterman, P.; Finley, J.; Han, J.; Zhang, P.; Hou, J. T.; Stiles, M. D.; Grutter, A. J.; Liu, L. Manipulation of coupling and magnon transport in magnetic metal-insulator hybrid structures. *Phys. Rev. Appl.* **2020**, *13*, 061002.
- (24) Fan, Y.; Finley, J.; Han, J.; Holtz, M. E.; Quarterman, P.; Zhang, P.; Safi, T. S.; Hou, J. T.; Grutter, A. J.; Liu, L. Resonant spin transmission mediated by magnons in a magnetic insulator multilayer structure. *Adv. Mater.* **2021**, *33*, 2008555.
- (25) Klingler, S.; Amin, V.; Geprägs, S.; Ganzhorn, K.; Maier-Flaig, H.; Althammer, M.; Huebl, H.; Gross, R.; McMichael, R. D.; Stiles, M. D.; Goennenwein, S. T. B.; Weiler, M. Spin-torque excitation of perpendicular standing spin waves in coupled YIG/Co heterostructures. *Phys. Rev. Lett.* **2018**, *120*, 127201.
- (26) Mohamad, H. J.; Shelford, L. R.; Aziz, M.; Al-Jarah, U. A. S.; Al-Saigh, R.; Valkass, R. A. J.; Marmion, S.; Hickey, B. J.; Hicken, R. J. Thermally induced magnetization dynamics of optically excited YIG/Cu/Ni<sub>81</sub>Fe<sub>19</sub> trilayers. *Phys. Rev. B: Condens. Matter Mater. Phys.* **2017**, 96, 134431.
- (27) Li, Y.; Cao, W.; Amin, V. P.; Zhang, Z.; Gibbons, J.; Sklenar, J.; Pearson, J.; Haney, P. M.; Stiles, M. D.; Bailey, W. E.; Novosad, V.; Hoffmann, A.; Zhang, W. Coherent spin pumping in a strongly coupled magnon-magnon hybrid system. *Phys. Rev. Lett.* **2020**, *124*, 117202.
- (28) Zhang, S. S.-L.; Zhang, S. Magnon mediated electric current drag across a ferromagnetic insulator layer. *Phys. Rev. Lett.* **2012**, *109*, 096603.
- (29) Rezende, S. M.; Azevedo, A.; Rodríguez-Suárez, R. L. Magnon diffusion theory for the spin Seebeck effect in ferromagnetic and antiferromagnetic insulators. *J. Phys. D: Appl. Phys.* **2018**, *51*, 174004.
- (30) Du, C.; der Sar, T. V.; Zhou, T. X.; Upadhyaya, P.; Casola, F.; Zhang, H.; Onbasli, M. C.; Ross, C. A.; Walsworth, R. L.; Tserkovnyak, Y.; Yacoby, A. Control and local measurement of the spin chemical potential in a magnetic insulator. *Science* **2017**, 357, 195–198
- (31) Brataas, A.; van Wees, B. J.; Klein, O.; de Loubens, G.; Viret, M. Spin insulatronics. *Phys. Rep.* **2020**, *885*, 1–27.
- (32) Ding, J.; Liu, T.; Chang, H.; Wu, M. Sputtering growth of low-damping yttrium-iron-garnet thin films. *IEEE Magn. Lett.* **2020**, *11*, 1–5.
- (33) Matsukura, F.; Tokura, Y.; Ohno, H. Control of magnetism by electric fields. *Nat. Nanotechnol.* **2015**, *10*, 209–220.
- (34) Manchon, A.; Železný, J.; Miron, I. M.; Jungwirth, T.; Sinova, J.; Thiaville, A.; Garello, K.; Gambardella, P. Current-induced spin-

orbit torques in ferromagnetic and antiferromagnetic systems. Rev. Mod. Phys. 2019, 91, 035004.